Photophysics

DOI: 10.1002/anie.201305536

A Strongly Emitting Liquid-Crystalline Derivative of $Y_3N@C_{80}$: Bright and Long-Lived Near-IR Luminescence from a Charge Transfer State**

Kalman Toth, Jennifer K. Molloy, Micaela Matta, Benoît Heinrich, Daniel Guillon, Giacomo Bergamini, Francesco Zerbetto, Bertrand Donnio,* Paola Ceroni,* and Delphine Felder-Flesch**

Dedicated to Professor Maurizio Prato on the occasion of his 60th birthday

Metal-containing fullerenes, and particularly trimetallic nitride template endohedral metallofullerenes (TNT-EMFs),[1] elicit increasing attention[2] not only for their fascinating structure and potential for stabilizing metallic nitrides, but also for their outstanding electronic and optical properties. TNT-EMFs are noteworthy electron acceptors.[3,4] They also possess larger absorption coefficients than C_{60} in the visible region, making them promising candidates for replacing the well-known phenyl C_{61} butyric acid methyl ester (PCBM) in bulk heterojunction (BHJ) solar cells.[5] They could then be used as potential auxiliary materials for singlet-exciton dissociation at the donor–acceptor interfaces, providing charge-transport pathways across the semiconducting layer.[6] Charge-carrier transport and light-emission efficiencies are closely related to the molecular organization and degree of ordering, for example, that found in the thin film morphology (nanostructuration). It is widely recognized that self-organization by the formation of low-dimensional liquid-crystalline (LC) phases is a key strategy for controlling the ordering and structuring of organic semiconductors because it helps to reduce or even suppress defect formation.[7] Chemical functionalization of TNT-EMFs[8] appears therefore to be an original and promising approach for reaching self-organization and obtaining processable materials. Although a wide number of LC fullerenes have been studied since the early 90s,[9] none of these studies concern the TNT-EMF family.

Herein, we report on the synthesis, functionalization, and characterization of the first TNT-EMF-based liquid crystal (**1**) and compare both mesomorphic and photophysical behaviors with the related C_{60} counterpart (**2**), synthesized as a model compound (Scheme 1). Both fullerene entities (C_{60} and $Y_3N@C_{80}$) are chemically linked to two oligo(phenylene ethynylene) (OPE) arms, which determine the self-organizing and absorbing properties.

Malonate bearing double OPE units (**dOPE**) or mono-brominated **dOPE** were reacted to the C_{60} and $Y_3N@C_{80}$

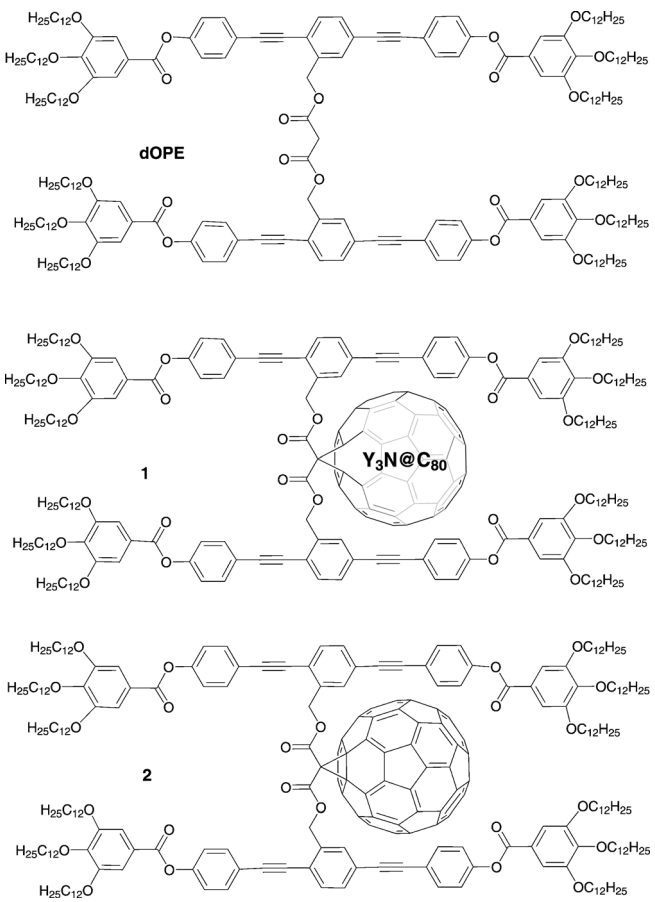

Scheme 1. Chemical structures of $Y_3N@C_{80}$-based (**1**) and C_{60}-based (**2**) dyads and their common malonate intermediate **dOPE**.

[*] Dr. K. Toth, Dr. B. Heinrich, Dr. D. Guillon, Dr. B. Donnio, Dr. D. Felder-Flesch
Institut de Physique et Chimie des Matériaux de Strasbourg
UMR CNRS UdS 7504
23 rue du loess BP 43, 67034 Strasbourg Cedex 2 (France)
E-mail: Bertrand.Donnio@ipcms.unistra.fr
Delphine.Felder@ipcms.unistra.fr
Dr. J. K. Molloy, M. Matta, Dr. G. Bergamini, Prof. F. Zerbetto, Prof. P. Ceroni
Dipartimento di Chimica "G. Ciamician", Universita' di Bologna
Via Selmi, 2, 40126 Bologna (Italy)
E-mail: paola.ceroni@unibo.it
francesco.zerbetto@unibo.it

[**] This research is supported by the European Commission through grant agreement DENDREAMERS (ITN Marie Curie) n°215884 and ERC StG (PhotoSi, 278912). We are also grateful to the CNRS and the University of Strasbourg.

Supporting information for this article is available on the WWW under http://dx.doi.org/10.1002/anie.201305536.

fullerenes, respectively, under classical Bingel reaction conditions (see the Supporting Information):[10] methanofullerene derivative **2** was produced in 84% yield, whereas TNT-EMF **1** was obtained with moderate yield owing to its lesser reactivity towards cyclopropanation. Indeed, smaller pyramidalization angles and longer bond lengths typify the carbon–carbon bonds of C_{80} relative to the reactive pyracylene-type site of C_{60}. This finding implies that electronic and geometric effects concur with the lower exohedral reactivity of C_{80}. Indeed, as previously described,[11] large excesses of both 1,8-diazabicyclo[5.4.0]undec-7-ene (DBU) and bromomalonate were necessary to obtain **1** in 20% yield after 2 h stirring in chlorobenzene and purification by preparative thin-layer chromatography.

Experimentally, both [5,6] and [6,6] types of double bonds can be potential reactive sites in TNT fullerenes, although the regioselectivity is usually very high.[2]

NMR spectroscopy is a powerful technique for distinguishing between these two addition patterns, but the low solubility of most of the TNT-EMF derivatives usually prevents their NMR characterization, and the use of ^{13}C-labeled samples or solvent mixtures with CS_2 are required. The presence of twelve long alkyl chains, however, enabled the complete NMR characterization of the $Y_3N@C_{80}$ derivative **1** in pure chloroform and confirmed that the product is a [6,6]-bridged fulleroid (see the Supporting Information).

The absorption spectra of **1** and **2** in toluene solution show the contribution of the two constituent chromophores: the band at 326 nm is mainly due to the OPE units, while the absorption at $\lambda > 380$ nm is characteristic of the fullerene core (Figure 1a). Notably, the molar absorption coefficient of **1** in the visible region is much higher than that of **2**, and the absorption extends up to 750 nm because of the endohedral fullerene core.

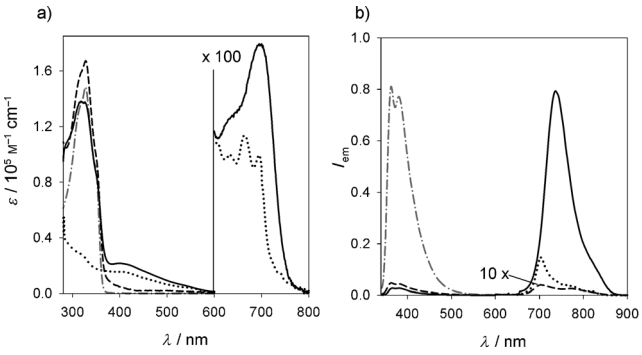

Figure 1. Absorption (a) and emission (b) spectra of **1** (——), **2** (– – –), **dOPE** (–•–•), and $Y_3N@C_{80}$ (•••••) in deaerated toluene solution at 298 K. $\lambda_{ex} = 325$ nm. The emission intensities are registered for iso-absorbing solutions at the λ_{ex}.

The emission spectra of **1** and **2** in deaerated toluene solutions (Figure 1b) show two bands: the first one at approximately 365 nm is due to the OPE moiety and is strongly quenched (>20 times) compared to the model compound **dOPE**, and the second one in the 680–900 nm region can be attributed to the fullerene core (Table 1). The quenching of the OPE fluorescence can be attributed to a 100% efficient energy transfer. Indeed, the same fullerene emission intensity was recorded upon excitation of iso-absorbing solutions of **1** at either 320 nm, where most of the light is absorbed by the pendant OPEs, or 405 nm, where only the fullerene absorbs light (Figure 1). The same result was observed for compound **2**. Therefore, the two OPE units act as extremely efficient light-harvesting antennae for the sensitization of the fullerene emission.

Table 1: Emission properties of **1**, **2**, **dOPE**, and $Y_3N@C_{80}$ in air-equilibrated or deaerated (values in brackets) toluene solution, unless otherwise noted.

	$T = 298$ K				$T = 77$ K[a]	
	λ [nm]	Φ_{em} [%]	τ [ns]	$\Phi(^1O_2)$	λ [nm]	τ [ms]
1	366	0.26 (0.26)	<0.8 (<0.8)	–	375	–[b]
	743	0.41 (8.0)	640 (16×10^3)	1.0	760	13
$Y_3N@C_{80}$	704	0.25 (1.1)	200 (780)	0.7	690	12×10^{-3}
dOPE	363	8.0	<0.8 (<0.8)	–	380 420	–[c] –[c]
2	363	0.35	<0.8	1.0	382	–[b]
	704	0.03	1.5		–[b]	–

[a] In toluene/ethanol 1:1 (v/v) rigid matrix. [b] The emission intensity is too low. [c] Multiexponential decay.

The most striking difference between the two derivatives concerns the fullerene core emission: in the case of **2**, a very weak fluorescence ($\Phi_{em} = 0.03\%$) with a lifetime of 1.5 ns is observed, as expected for C_{60} derivatives. By contrast, compound **1** exhibits outstanding luminescence properties in the near-IR region, even better than the nonfunctionalized model $Y_3N@C_{80}$. As reported in Table 1, the emitting excited state of **1** is: 1) slightly lower in energy compared to the nonfunctionalized endohedral fullerene, 2) quite highly emitting (8.0% in deaerated solution), 3) extremely long-lived (16 μs at 298 K, 20 times higher than $Y_3N@C_{80}$, and 13 ms at 77 K), and 4) highly sensitive to the presence of dioxygen in fluid solution (see below). The same emission band is observed in the solid phase, in both the amorphous phase and the LC mesophase, with strong quenching by dioxygen.

Dioxygen efficiently quenches the emission of **1** in solution as well, with a rate constant $k_q = 8\times10^8\,M^{-1}s^{-1}$. This value is slightly lower than that of the pristine $Y_3N@C_{80}$ ($k_q = 2\times10^9\,M^{-1}s^{-1}$), a result consistent with an embedding of the fullerene core in the OPE units of **1**. Quenching by dioxygen (Scheme 2) leads to sensitization of $^1O_2$ emission at 1270 nm with a quantum yield of 1.0 and 0.7 for **1** and $Y_3N@C_{80}$, respectively (Table 1). The fluorescence of compound **2** is not quenched by dioxygen because of its very short lifetime, which prevents dynamic quenching. However, **2** can sensitize $^1O_2$ through its lowest lying triplet excited state (see the

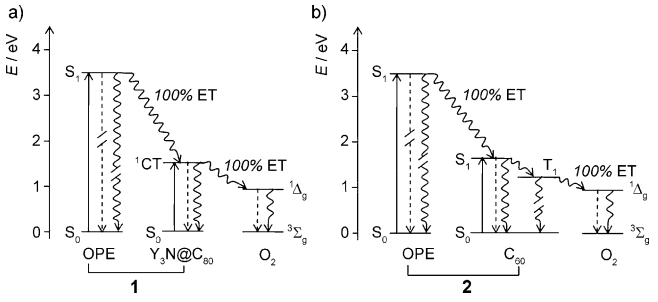

Scheme 2. Energy level diagrams showing the most relevant radiative (straight lines) and nonradiative (wavy lines) processes for **1** (a) and **2** (b). The excited states not relevant to the present discussion have been omitted for clarity. ET = energy transfer.

Supporting Information) with efficiency close to 1, as expected for C_{60} derivatives.

Quenching of the luminescence of **1** has been observed upon addition of ferrocene, with $k_q = 6 \times 10^9\ M^{-1} s^{-1}$, a value lower than that of $Y_3N@C_{80}$ ($k_q = 1 \times 10^{10}\ M^{-1} s^{-1}$) because of the embedding effect of the OPE units of **1**. The quenching occurs by photoinduced electron transfer from ferrocene to **1** as a result of the fact that the ferrocene is easy to reduce but not to oxidize and it has no excited state lower than that of **1**.

To further explore the nature of the long-lived emitting excited state, density functional theory (DFT) calculations were performed (Figure 2) on $Y_3N@C_{80}$ and compared to those obtained for $Sc_3N@C_{80}$, a closely related EMF that has a similar absorption spectrum but does not emit.

The DFT-optimized geometries at B3LYP/6-311G*/ECP level agreed with the structures proposed earlier.[12] Both

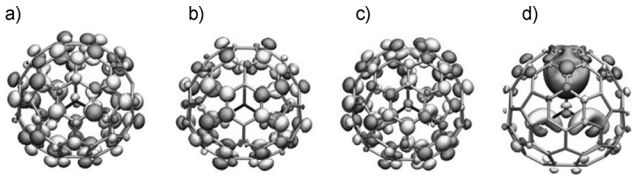

Figure 2. a) HOMO of $Sc_3N@C_{80}$, b) HOMO of $Y_3N@C_{80}$, c) LUMO of $Sc_3N@C_{80}$, d) LUMO of $Y_3N@C_{80}$.

Sc_3N and Y_3N are planar. The amount of intramolecular charge transfer is larger for $Y_3N@C_{80}$ than $Sc_3N@C_{80}$, with the Y_3N-doped cage receiving 3.84(4.99) electrons while the corresponding value for the Sc_3N-doped cage is 2.98(3.41) with the B3LYP(HSE06) functional. The large charge transfer values suggest that molecule–cage Coulomb interactions play an important role in the structure and properties of these endohedral clusters. Further time-dependent DFT and ZINDO/S calculations showed that the lowest electronically excited singlet state S_1 of both $Sc_3N@C_{80}$ and $Y_3N@C_{80}$ is mainly a HOMO–LUMO transition. The HSE06/6-311G*, CAM-B3LYP/6-311G*, and ZINDO/S results locate S_1 of $Y_3N@C_{80}$ at 2.02, 2.55, and 1.72 eV. For $Sc_3N@C_{80}$, the corresponding values are 1.72, 2.20, and 1.74 eV. A crucial difference between $Sc_3N@C_{80}$ and $Y_3N@C_{80}$ emerges when the molecular orbitals involved in S_1 are inspected visually. Figure 2 shows the HOMOs and LUMOs of the two endohedral clusters. In the nonemitting, short-lived S_1 state of $Sc_3N@C_{80}$,[13] the electron excitation is spread over the entire molecule: both the cage and the endohedrally confined Sc_3N participate in the excitation. In the emitting, long-lived S_1 state of $Y_3N@C_{80}$, the electron excitation has a strong charge-transfer character, from the carbon cage to the endohedrally trapped Y_3N. The peculiar photophysical differences between $Sc_3N@C_{80}$ and $Y_3N@C_{80}$ are now easily accounted for. The electron excitation to the cage-screened Y_3N leads to the long lifetime of S_1 and inhibits the typical fullerenic deactivation pathway characterized by very low emission quantum yields. Our findings agree with previous calculations that showed the charge-transfer character of S_1 of $Y_3N@C_{80}$.[14]

Fullerene adducts **1** and **2** are amorphous in the pristine state, but they self-organize into a LC mesophase during the first heating (at ca. 70 °C for **1** and ca. 80 °C for **2**). The mesophase is retained upon cooling to room temperature, and also recovered on cooling after a further heating beyond the isotropization temperature, at approximately 80 °C for **1** and 100 °C for **2** (see the Supporting Information).

A complete elucidation of the self-organizing behavior of **1** and **2** was achieved by using small-angle X-ray scattering (SAXS; Table 2 and see the Supporting Information). Columnar mesophases were readily recognized from diffraction patterns, which are composed of the usual diffuse scattering at

Table 2: Geometrical parameters of mesophases obtained from X-ray data at 20 °C.

	2D lattice	
Sample Phase V_{mol} [Å^3][a]	a [Å] × b [Å][b] A [Å^2] (Z_{col})[c]	S_{col} [Å^2][d] N_{ful}[e] h_{col} [Å][f]
1	80.9 × 46.7	1889
Col_{hex}	3778 (2)	3
6502		10.3
2	80.2 × 46.3;	1857
Col_{rec}	3713 (2)	3
6231		10.1

[a] Calculated molecular volume. [b] Lattice parameters of the columnar phase. [c] 2D lattice area (A) (hexagonal lattice doubled); number of columns per lattice (Z_{col}). [d] Cross-section area of a single column ($S_{col} = A/Z_{col}$). [e] Fullerenes imposed a repeating thickness of $h_{col} = N_{ful} V_{mol}/S_{col} \approx 10$ Å, leading to the integer fullerene number $N_{ful} = 3$. [f] h_{col} recalculated considering N_{ful} to be equal to 3.

4.5 Å that is indicative of the liquid-like lateral packing of the aliphatic chains and mesogenic OPE cores, and of up to 4 sharp reflections with the spacing ratio $1:\sqrt{3}:2:\sqrt{7}$ in the small-angle region that are indicative of a 2D lattice with hexagonal geometry (the reflection at $\sqrt{7}$ was not detected for **1**, see the Supporting Information). Since no further small-angle reflection is visible in the patterns of **1**, the mesophase is assigned to Col_{hex}. One additional, weak signal located at twice the spacing of the first reflection of the series is detected in the patterns of **2**, and the real lattice therefore includes

several hexagonal cells, presumably under the effect of small shifts in orientation and/or position between neighboring columns, induced by its more symmetrical molecular structure (with respect to that of **1**).[15] The doubling of the hexagonal sublattice then generates a primitive rectangular lattice containing two columns, assigned to a Col_{rec} phase with pseudohexagonal geometry.[16]

Except for the lattice doubling, both columnar structures appear overall to be very similar. The grafting of a C_{60} or TNT-EMF C_{80} unit onto the central bridge of **dOPE** generates an unusual triblock architecture, which leads to the triple microsegregation of fullerenes, mesogenic cores, and chains into different zones separated by interfaces constraining the organization, similar to the situation in the complex "multicolor tiling" mesophases generated by polyphilic systems.[17] A further similarity between both organizations is in the size of the columns: their similar cross-sections (S_{col}); about 1.5% larger in **1**, and in both cases nearly independent of temperature (see the Supporting Information), lead to slice thicknesses ($h_{mol} = V_{mol}/S_{col}$)[16,18] of between 3.4 and 3.6 Å. These values represent about one third of the distance between the nearest-neighbor fullerenes obtained from crystalline phases (about 10 and 11 Å, for C_{60} and C_{80}, respectively) and column cross-sections therefore contain an average $N_{ful} = 3$ (Table 2 and see the Supporting Information). This suggests the image of successive molecular plates with a core of three interacting fullerenes stacked into columns with an alternating 60° rotation, yielding a strand of hexagonally close packed bowls, as schematized in Figure 3 (see the Supporting Information). The associated three pairs of OPE mesogens are pressed against the fullerene strands, and owing to the short spacers are spatially constrained and form a sort of separating two-dimensional net between the fullerene strands and the aliphatic chain tubes, to give a structure reminiscent of a Kagome lattice (Figure 3a): a periodic 2D tiling of regular hexagons (filled by hcp stacked fullerenes) and triangles (filled by the molten aliphatic chains) in a 1:2 ratio.[19] The lateral mesogens may adopt various orientations around a preferential one that lies between the parallel and perpendicular limit cases, but likely closer to the perpendicular orientation (see the Supporting Information).

Optimization of the structure of a supercell made by nine molecules of **1** using a calculation method employed before[20] yielded a cell of 78.8 × 45.5 Å (Figure 3b), which compares well with the value obtained from the X-ray data of 80.9 × 46.7 Å. The calculations also provide a value of h_{col} (ca. 11 Å) that is in agreement with X-ray data.

In conclusion, we have synthesized the first example of a liquid-crystalline derivative of $Y_3N@C_{80}$ that shows good solubility and remarkable photophysical properties: OPE units act as 100% efficient light-harvesting antennae to sensitize a bright and long-lived fullerene core emission. These luminescence properties are retained in the mesophase and, coupled to a quite strong absorption in the visible region extending up to 750 nm, open up a variety of potential applications, for example near-IR luminescent sensors with time-gated detection to shut down fluorescence of the matrix or competing species. The grafting of the mesomorphic **dOPE** onto the fullerenes promotes mesomorphism in the fullerene

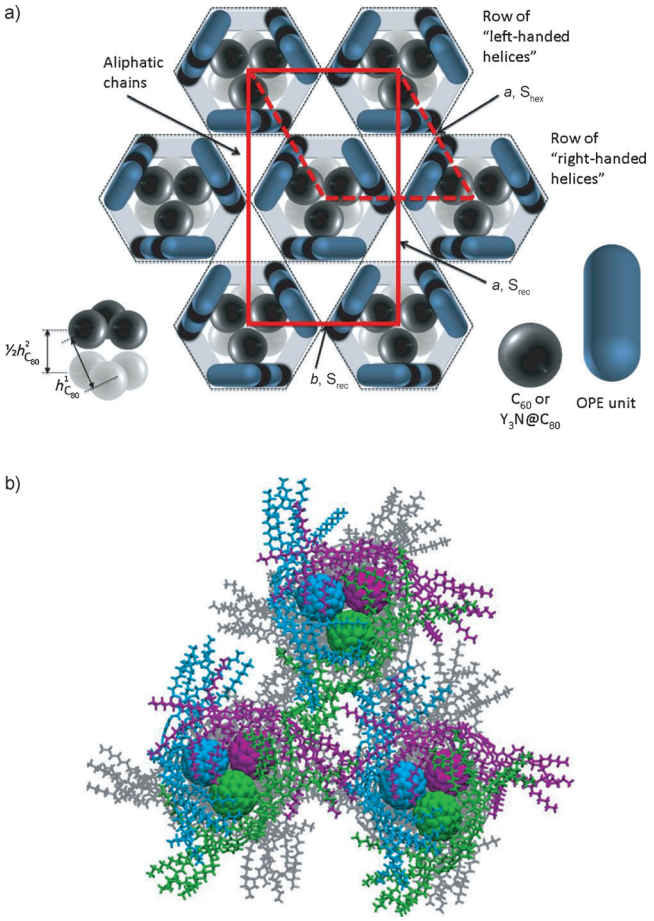

Figure 3. a) Schematic view of the supramolecular packing of adducts **1** and **2** (solid and dotted red lines: S_{hex} and S_{rec} lattices of the Col_{hex} and Col_{rec} phases, respectively; dotted-black lines: Kagome lattice). b) Computer modeling of a supercell of nine molecules of **1** arranged as in (a). The different colors are used to assist the eye.

adducts, with the induction of columnar phases resulting from the triple segregation between the fullerene (core), mesogens (walls), and chains (continuous medium) according to a Kagome lattice. Such a novel design paradigm could be further exploited to produce a unique class of lanthanido-mesogens with original luminescent and magnetic properties.[21]

Received: June 27, 2013
Published online: October 7, 2013

Keywords: density functional calculations · endohedral cluster fullerenes · liquid crystals · metallomesogens · photophysics

[1] a) S. Stevenson, G. Rice, T. Glass, K. Harich, F. Cromer, M. R. Jordan, J. Craft, E. Hadju, R. Bible, M. M. Olmstead, K. Maitra, A. J. Fisher, A. L. Balch, H. C. Dorn, *Nature* **1999**, *401*, 55–57; b) L. Dunsch, S. F. Yang, *Small* **2007**, *3*, 1298–1320; c) J. Zhang, S. Stevenson, H. C. Dorn, *Acc. Chem. Res.* **2013**, *46*, 1548–1557.

[2] M. N. Chaur, F. Melin, A. L. Ortiz, L. Echegoyen, *Angew. Chem.* **2009**, *121*, 7650 – 7675; *Angew. Chem. Int. Ed.* **2009**, *48*, 7514 – 7538.

[3] a) J. Aihara, *J. Phys. Chem. A* **2002**, *106*, 11371 – 11374; b) C.-R. Wang, T. Kai, T. Tomiyama, T. Yoshida, Y. Kobayasi, E. Nishibori, M. Takata, M. Sakata, H. Shinohara, *Nature* **2000**, *408*, 426 – 427; c) J. C. Duchamp, A. Demortier, K. R. Fletcher, D. Dorn, E. B. Iezzi, T. Glass, H. C. Dorn, *Chem. Phys. Lett.* **2003**, *375*, 655 – 659; d) M. Krause, L. Dunsch, *ChemPhysChem* **2004**, *5*, 1445 – 1449.

[4] a) J. R. Pinzón, M. E. Plonska-Brzezinska, C. M. Cardona, A. J. Athans, S. S. Gayathri, D. M. Guldi, M.-A. Herranz, N. Martin, T. Torres, L. Echegoyen, *Angew. Chem.* **2008**, *120*, 4241 – 4244; *Angew. Chem. Int. Ed.* **2008**, *47*, 4173 – 4176; b) J. R. Pinzón, D. C. Gasca, S. G. Sankaranarayanan, G. Bottari, T. Torres, D. M. Guldi, L. Echegoyen, *J. Am. Chem. Soc.* **2009**, *131*, 7727 – 7734; c) R. B. Ross, C. M. Cardona, F. B. Swain, D. M. Guldi, S. G. Sankaranarayanan, E. Van Keuren, B. Holloway, M. Drees, *Adv. Funct. Mater.* **2009**, *19*, 2332 – 2338.

[5] a) Y. Takano, S. Obuchi, N. Mizorogi, R. García, M.-A. Herranz, M. Rudolf, S. Wolfrum, D. M. Guldi, N. Martín, S. Nagase, T. Akasaka, *J. Am. Chem. Soc.* **2012**, *134*, 16103 – 16606; b) Y. Takano, S. Obuchi, N. Mizorogi, R. García, M.-A. Herranz, M. Rudolf, D. M. Guldi, N. Martín, S. Nagase, T. Akasaka, *J. Am. Chem. Soc.* **2012**, *134*, 19401 – 19408.

[6] a) M. Liedtke, A. Sperlich, H. Kraus, A. Baumann, C. Deibel, M. J. M. Wirix, J. Loos, C. M. Cardona, V. Dyakonov, *J. Am. Chem. Soc.* **2011**, *133*, 9088 – 9094; b) R. B. Ross, C. M. Cardona, D. M. Guldi, S. G. Sankaranarayanan, M. O. Reese, N. Kopidakis, J. Peet, B. Walker, G. C. Bazan, E. Van Keuren, B. C. Holloway, M. Drees, *Nat. Mater.* **2009**, *8*, 208 – 212.

[7] a) S. Sergeyev, W. Pisula, Y. V. Geerts, *Chem. Soc. Rev.* **2007**, *36*, 1902 – 1929; b) W. Pisula, M. Zorn, J. Y. Chang, K. Müllen, R. Zentel, *Macromol. Rapid Commun.* **2009**, *30*, 1179 – 1202; c) M. O'Neill, S. M. Kelly, *Adv. Mater.* **2011**, *23*, 566 – 584.

[8] X. Lu, T. Akasaka, S. Nagase, *Chem. Commun.* **2011**, *47*, 5942 – 5957.

[9] a) H. Mamlouk, B. Heinrich, C. Bourgogne, B. Donnio, D. Guillon, D. Felder-Flesch, *J. Mater. Chem.* **2007**, *17*, 2199 – 2205; b) S. Campidelli, P. Bourgun, B. Guintchin, J. Furrer, H. Stoeckli-Evans, I. M. Saez, J. W. Goodby, R. Deschenaux, *J. Am. Chem. Soc.* **2010**, *132*, 3574 – 3581; c) T. N. Y. Hoang, D. Pociecha, M. Salamonczyk, E. Gorecka, R. Deschenaux, *Soft Matter* **2011**, *7*, 4948 – 4953; d) J. Vergara, J. Barberá, J.-L. Serrano, M. Blanca Ros, N. Sebastián, R. de La Fuente, D. O. López, G. Fernández, L. Sánchez, N. Martín, *Angew. Chem.* **2011**, *123*, 12731 – 12736; *Angew. Chem. Int. Ed.* **2011**, *50*, 12523 – 12528; e) Y. Matsuo, A. Muramatsu, Y. Kamikawa, T. Kato, E. Nakamura, *J. Am. Chem. Soc.* **2006**, *128*, 9586 – 9593; f) R. Deschenaux, B. Donnio, D. Guillon, *New J. Chem.* **2007**, *31*, 1064 – 1073.

[10] C. Bingel, *Chem. Ber.* **1993**, *126*, 1957 – 1959.

[11] C. M. Cardona, A. Kitaygorodskiy, L. Echegoyen, *J. Am. Chem. Soc.* **2005**, *127*, 10448 – 10453.

[12] L.-H. Gan, R. Yuan, *ChemPhysChem* **2006**, *7*, 1306 – 1310.

[13] J. R. Pinzón, C. M. Cardona, M.-A. Herranz, M. E. Plonska-Brzezinska, A. Palkar, A. J. Athans, N. Martin, A. Rodriguez-Fortea, J. M. Poblet, G. Bottari, T. Torres, S. S. Gayathri, D. M. Guldi, L. Echegoyen, *Chem. Eur. J.* **2009**, *15*, 864 – 877.

[14] R. Valencia, A. Rodriguez-Fortea, A. Clotet, C. de Graaf, M. N. Chaur, L. Echegoyen, J. M. Poblet, *Chem. Eur. J.* **2009**, *15*, 10997 – 11009.

[15] J. Grolik, L. Dudek, J. Eilmes, A. Eilmes, M. Gorecki, J. Frelek, B. Heinrich, B. Donnio, *Tetrahedron* **2012**, *68*, 3875 – 3884.

[16] F. Morale, R. W. Date, D. Guillon, D. W. Bruce, R. L. Finn, C. Wilson, A. J. Blake, M. Schröder, B. Donnio, *Chem. Eur. J.* **2003**, *9*, 2484 – 2501.

[17] a) C. Tschierske, *Chem. Soc. Rev.* **2007**, *36*, 1930 – 1970; b) C. Tschierske, *Top. Curr. Chem.* **2012**, *318*, 1 – 108.

[18] B. Donnio, B. Heinrich, H. Allouchi, J. Kain, S. Diele, D. Guillon, D. W. Bruce, *J. Am. Chem. Soc.* **2004**, *126*, 15258 – 15268.

[19] B. Glettner, F. Liu, X. Zeng, M. Prehm, U. Baumeister, M. Walker, M. A. Bates, P. Boesecke, G. Ungar, C. Tschierske, *Angew. Chem.* **2008**, *120*, 9203 – 9206; *Angew. Chem. Int. Ed.* **2008**, *47*, 9063 – 9066.

[20] T. W. Chamberlain, R. Pfeiffer, H. Peterlik, H. Kuzmany, F. Zerbetto, M. Melle-Franco, L. Staddon, N. R. Champness, G. A. D. Briggs, A. N. Khlobystov, *Small* **2008**, *4*, 2262 – 2270.

[21] a) K. Binnemans, C. Görller-Walrand, *Chem. Rev.* **2002**, *102*, 2303 – 2346; b) C. Piguet, J.-C. G. Bünzli, B. Donnio, D. Guillon, *Chem. Commun.* **2006**, 3755 – 3768.

